



ELSEVIER

Available online at [www.sciencedirect.com](http://www.sciencedirect.com)

SCIENCE @ DIRECT®

Physica A 351 (2005) 175–183

PHYSICA A

[www.elsevier.com/locate/physa](http://www.elsevier.com/locate/physa)

# Auditory two-tone suppression from a subcritical Hopf cochlea

R. Stoop<sup>a,\*</sup>, W.-H. Steeb<sup>b</sup>, J.C. Gallas<sup>c</sup>, A. Kern<sup>a</sup>

<sup>a</sup>*Institute of Neuroinformatics ETHZ/UNIZH, Winterthurerstr. 190, 8057 Zürich, Switzerland*

<sup>b</sup>*International School of Scientific Computing, Johannesburg University, Auckland, Johannesburg, South Africa*

<sup>c</sup>*Instituto da Física, Universidade Federal Do Rio Grande Do Sul (UFRGS), 91501-970 Porto Alegre, Brazil*

Received 5 October 2004

Available online 1 January 2005

---

## Abstract

Cochlear two-tone suppression is the dominant contrast-sharpening phenomenon of hearing and provides a decisive test for the correct implementation of hearing nonlinearities in models of the cochlea. Although *critically* tuned Hopf amplifiers were shown recently to be fruitful models of intricate phenomena in the physiology of the human ear, we find that only a model based on *subcritical* Hopf amplifiers is capable of reproducing physiologically measured two-tone suppression data adequately. In addition, we provide a detailed explanation of the two-tone suppression phenomenon, including its quantitative characterization.

© 2004 Elsevier B.V. All rights reserved.

PACS: 43.64.Bt; 43.64.Kc

---

## 1. Introduction

The determination of the working principles of the mammalian cochlea is a great challenge from a scientific, technological, and medical point of view. Motivated by cochlear anatomy, Helmholtz was the first to come up with a simple cochlea model

---

\*Corresponding author. Tel.: +41 16353063.

E-mail address: [ruedi@ini.phys.ethz.ch](mailto:ruedi@ini.phys.ethz.ch) (R. Stoop).

URL: <http://stoop.net/group>.

by hypothesizing a place–frequency mapping along the cochlear duct [1]. A specific place in the cochlea would react to a particular frequency only, much like the strings on a piano (the so-called tonotopic principle). Half a century later, von Békésy's [2] physiological measurements proved the essentials of Helmholtz's theory. He observed travelling waves along the cochlear basilar membrane (BM) that assumed maximum amplitude at places determined by the frequencies of the stimulating tones. Later, hydrodynamic models of the cochlea explained these findings from first principles [3].

In the following decades, physiological measurements revealed a number of hearing phenomena that failed to be explained by means of this linear theory, the most prominent of which is BM two-tone suppression [4–6]. If more than one tone is presented to the cochlea, this results in an attenuated response to the tones. By completely suppressing the small contributions, the representation of the large components in a sound spectrum is significantly enhanced.

It is generally assumed [7] that two-tone suppression is closely related with the main source of hearing nonlinearity, the ability of the cochlea to actively influence the state of the cochlear fluid. As the most striking manifestation of these *active* cochlea processes [8], the cochlea may generate fluid waves even in the absence of external stimulation. Using the reversed usual pathway, the fluid wave converts to a sound wave (called otoacoustic emissions [9]), which can be measured by ear-canal microphones. When the active processes are inactivated, two-tone suppression ceases to work [10,11], indicating a close relationship between the two phenomena. Eguiluz et al. [12] were the first to point out that the active processes could be incorporated into cochlea modelling by means of Hopf oscillators. The actual implementation of this concept within the known properties of the cochlea, however, was left open. Hopf-type response in amphibian hair cells [13], the ancestors of the mammalian outer hair cells, indicated that the active mammalian hearing process, which originates in the mechano-sensory outer hair cells attached to the BM, is also of Hopf type. In this contribution, we show that a biophysically motivated implementation of Hopf amplifiers correctly reproduces physiological two-tone suppression and, additionally, provides a detailed and accurate explanation of the underlying mechanism.

## 2. Hopf–type active amplification

The generic Hopf system describing active amplification in hearing has the form [12]

$$\dot{z} = (\mu + i\omega_0)z - |z|^2z + Fe^{i\omega t}, \quad z(t) \in \mathbb{C}. \quad (1)$$

In this equation,  $\omega_0(x)$  is the frequency for which the measurement at location  $x$  along the cochlear duct yields the maximal response (the tonotopic principle).  $\omega$  is the frequency of the external stimulation,  $z(t)$  can be considered the amplification of the input signal  $F(t)$ . In the absence of external forcing ( $F = 0$ ), the equation displays a Hopf bifurcation [14]. For bifurcation parameter  $\mu < 0$ , the solution  $z(t) = 0$  is a

stable fixed point, which for  $\mu > 0$  becomes unstable and is replaced by a stable limit-cycle  $z(t) = \sqrt{\mu}e^{i\omega_0 t}$ . The steady-state solution for periodic forcing is obtained with the ansatz  $z(t) = Re^{i\omega t + i\phi}$ , where a 1:1 locking between signal and system is assumed. The response amplitude  $R$  is then determined from a cubic equation in  $R^2$ ,

$$F^2 = R^6 - 2\mu R^4 + [\mu^2 + (\omega - \omega_0)^2]R^2. \tag{2}$$

The detailed understanding of the input–output relation provided by this equation will be the basis for understanding two-tone suppression. For  $\mu = 0$  and close to resonance  $\omega = \omega_0$ , the response  $R = F^{1/3}$  emerges, which forces the gain  $G = R/F = F^{-2/3}$  to increase towards infinity as  $F$  approaches zero. This implies a compressive nonlinearity, for any stimulus size. For  $\mu < 0$  and still close to resonance, for weak stimuli  $F$  we obtain the response  $R = -F/\mu$ . As  $F$  increases, the term  $R^6$  in Eq. (2) can no longer be neglected, and as  $R^6 \approx \mu^2 R^2$ , the compressive nonlinear regime is entered. The transition occurs at  $F_{cnl} \approx (-\mu)^{3/2}$ . Therefore, for weak stimuli  $F$ , the response  $R$  is nearly linear, whereas for moderate stimuli the differential gain  $dR/dF$  decreases with increasing stimulus intensity. Away from the resonance, the last term in Eq. (2) dominates. In this case, the response is linear for every input, since  $R \approx F/|\omega - \omega_0|$ .

### 3. Two frequencies response

To investigate the effects generated by the presence of two tones  $(F_t, \omega_t)$  and  $(F_s, \omega_s)$ , we use the Fourier series ansatz

$$z(t) = R_t \exp(i\omega_t t + i\phi_t) + R_s \exp(i\omega_s t + i\phi_s) + \sum_{n,m} R_{n,m} \exp(i\omega_{n,m} t + i\phi_{n,m}),$$

where  $\{R_s, R_t\}$  are the response components of frequencies  $\{\omega_s, \omega_t\}$ , the dominant frequency components of the input. The tone indexed by  $t$  represents a test tone that, in the presence of a suppressor tone, indexed by  $s$ , is reduced (as we will show). Note, however, that the roles of the test and the suppressor tone are interchangeable. The frequencies  $\omega_{n,m} := n\omega_t + m\omega_s$ ,  $n, m \in \mathbb{Z}^+$ , represent higher harmonics of the input frequencies, called the combination tones [12].

The Fourier series ansatz is inserted into the generic Hopf equation and the contributions belonging to the frequency  $\omega_{n,m} = n\omega_t + m\omega_s$  are collected. The first contributions are  $R_{n,m} \sim R_t^n R_s^m$ , which suggests to speak of  $|n| + |m|$  as the order of  $R_{n,m}$ . If  $k - l = n$  and  $q - r = m$ , the Hopf nonlinearity will generate contributions to  $\omega_{n,m}$  that are based on frequencies  $(k\omega_t - l\omega_t) + (q\omega_s - r\omega_s)$ , but are of higher order  $|k| + |l| + |q| + |r|$ . When inserted into the Hopf nonlinearity, we can see that only odd orders are generated and that the lowest contributions from  $R_t$  and  $R_s$  are of order three. Collecting them yields

$$i\omega_k R_k = (\mu + i\omega_0)R_k - R_k(|R_k|^2 + 2|R_l|^2) + F_k \exp(-i\phi_k), \tag{3}$$

where  $k \neq l \in \{t, s\}$ . After isolating the phases and multiplying by their complex conjugates, we obtain

$$F_k^2 = R_k^6 - 2(\mu - 2R_l^2)R_k^4 + [(\mu - 2R_l^2)^2 + (\omega_k - \omega_0)^2]R_k^2 \quad (4)$$

with  $k \neq l \in \{t, s\}$ . Comparison with the Hopf response, Eq. (2) shows that these expressions are of the same form, with *effective* bifurcation parameters

$$\mu_{eff,k} = \mu - 2R_l^2, \quad k \neq l \in \{t, s\}. \quad (5)$$

In this way, the presence of a second tone is solely reflected in a pair of changed bifurcation parameters  $\mu_{eff,k}$ .

To model the whole cochlea, all active contributions are locally injected into the cochlea and combined with the passive hydrodynamic waves elicited by the stimulations. In Ref. [15], it was shown that this system can be described by a differential equation for one-dimensional energy density,  $e(x, \omega)$ ,

$$\frac{\partial e(x, \omega)}{\partial x} = -\frac{1}{v_G(x, \omega)} \left[ \frac{\partial v_G(x, \omega)}{\partial x} + d(x, \omega) \right] e(x, \omega) + \frac{a(x, e(x, \omega), \omega)}{v_G(x, \omega)}, \quad (6)$$

where  $d$  is the dissipation, counteracted by the power  $a$  delivered by the active process and  $v_G$  is the group velocity. The origin of this equation is in the steady-state situation, where an energy-balance argument [16] between dissipation and active amplification applies (for a detailed biophysical derivation of the model see Ref. [15], where it is also shown how second-order couplings [17] fine-tune the response). The active power  $a(\cdot)$  is determined from the fact that Hopf oscillators active at location  $x$  deliver a force whose amplitude is proportional to the Hopf response  $R$ , cf. Eq. (2),

$$a(e, x, \omega) \sim (R(\sqrt{e(x, \omega)}))^2. \quad (7)$$

A great advantage of this biophysically motivated cochlea model is that its results can be compared directly with physiological measurements. The locally generated forces lead [15] to a BM displacement

$$A(x, \omega) = (2e(x, \omega)/E(x))^{1/2}, \quad (8)$$

where  $E(x)$  is the exponentially decaying BM stiffness. Eqs. (6)–(8) establish the connection between the cochlea differential equation and physiological measurements.

#### 4. Two-tone suppression

For single tones, with realistic biophysical parameters, our model leads to plausible responses only when subcritical tuning  $\mu < 0$  is used (see concluding discussion). In this case, the simulation results closely match the physiological measurements, even in the simplest variant of the model. Moreover, also the responses obtained for two-tone suppression coincide with the physiological data, up

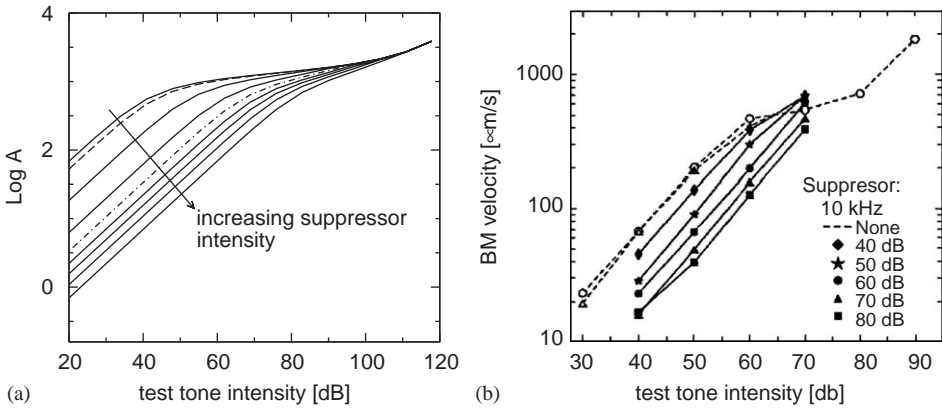


Fig. 1. High-side suppression: (a) Model response at resonance. Suppressor intensities from 10 to 110 dB, in steps of 10 dB. The 10, 20, and 30 dB lines coincide ( $\omega_t/2\pi = 0.9$  kHz,  $\omega_s/2\pi = 1.0$  kHz). (b) Experimental measurements [10] ( $\omega_t/2\pi = 8$  kHz).

to measurement accuracy (Fig. 1). To obtain this agreement, only the dB-scale origin and the proportionality constant in Eq. (7), which determines the gain and the width of the compressive nonlinearity, had to be chosen appropriately. In the model and in the experimental results alike, low-dB BM input–output curves slowly detach from the zero suppressor curve, staying in its neighborhood up to an intensity of 30 dB. This regime is followed by a regime of strong suppressor efficacy (indicated by large inter-curve distances), terminating in a regime of strongly reduced suppressor efficacy.

We now show that it is possible to qualitatively and quantitatively understand these results from the Hopf response in Eq. (4). To this end, we shall identify the BM response  $A$  with the Hopf response  $R$ , and the stimulation intensity  $I$  with the square of the forcing,  $F^2$ . The top curves of Fig. 1, for which two-tone suppression is virtually absent, express the Hopf-like response of the cochlea obtained for the test tone alone. A region of linear response for weak stimulation transforms at moderate signal intensities into the compressive nonlinearity characteristic for mammalian hearing, which terminates in the passive cochlea behavior obtained from Fig. 3a by plotting the BM peak responses as a function of stimulus intensity). Because of the interchangeable role of the test and the suppressor tone, the equivalent situation emerges when a fixed weak test-tone, which does not suppress the suppressor tone, is confronted with an increasing suppressor intensity. As a function of the latter, the BM displacement also shows the typical Hopf behavior. Displaying  $\log(A)$  as a function of the suppressor intensity yields Fig. 2a, which has similarity with the experimental data. The following detailed discussion will be restricted to high-side suppression. Repeating the arguments for low-side suppression is redundant.

When the suppressor is turned on with sufficiently weak intensity  $F_s$ , we are in the linear regime  $R_s \sim F_s$ . This implies  $R_s^2 \ll |\mu|$ , leading to  $\mu_{eff,t} \approx \mu$ , so that the generated response curve is confined to the close vicinity of the suppressor-free case.

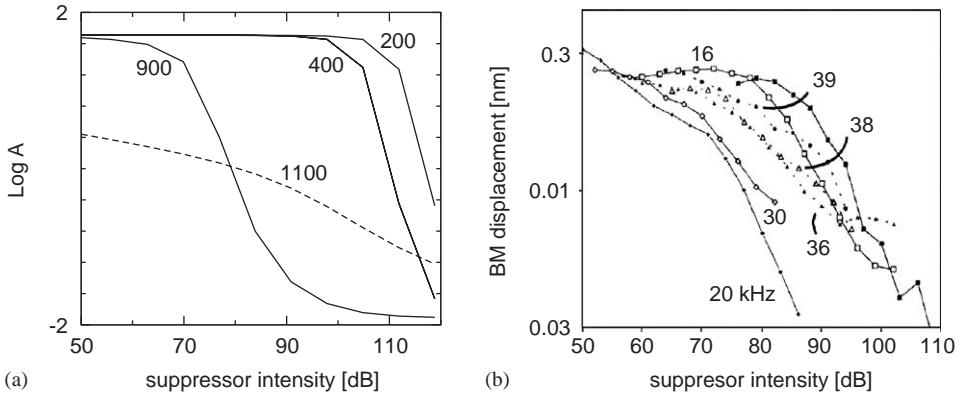


Fig. 2. Low-side suppression: (a) Model ( $\omega_t/2\pi = 1$  kHz). (b) Experimental measurements [11], where the labels indicate the suppression frequencies. The dotted 36, 38, 39 kHz suppression curves (and, for comparison, the dashed 1100 Hz-curve in panel (a)), relate to high-side suppression ( $\omega_t/2\pi = 34$  kHz). The high-side suppression curves demonstrate how the nonlinear compressive regime leads to a more moderate dependence of the test tone response on the suppressor intensity.

Moreover, the change of the bifurcation parameter  $\mu_{eff,t}$  as a function of  $F_s$  will be rather slow. Only if  $2R_s^2$  becomes comparable to  $\mu$  (dashed curve in Fig. 1a), the suppressor unfolds its efficacy. When  $2R_s^2$  dominates, we observe a linear logarithmic suppression. Finally, when the suppressor runs in its compressive nonlinearity (dashed-dotted curve), its efficacy slows down, ending in another regime of linear logarithmic suppression, with spacings reduced by about a factor of three.

## 5. Suppression laws

These observations can be made rigorous and quantitative. We will focus on the (logarithmic) linear test-tone regime, where the identification  $A_t \sim \sqrt{e} \sim R_t$  can be rigorously established from the formal solution of the cochlea equation. For weak stimulations  $F_t$  we have

$$R_t \approx \frac{F_t}{\mu_{eff,t}} = \frac{F_t}{\mu - 2R_s^2}. \quad (9)$$

Upon increasing the suppressor amplitude from  $F_s(1)$  to  $F_s(2)$ , the suppression increases by

$$\Delta_s = \log \frac{A_t(F_s(1))}{A_t(F_s(2))} \sim \log \frac{\mu - 2R_s(2)^2}{\mu - 2R_s(1)^2}. \quad (10)$$

Choosing  $F_s(1) = 0$  (zero suppressor stimulation), we obtain the onset behavior

$$\Delta_s(\text{ons}) \sim \log \frac{\mu - 2R_s(2)^2}{\mu} \approx -\frac{2R_s(2)^2}{\mu}. \quad (11)$$

Since for weak stimulations  $F_s$  we have  $R_s^2 \sim F_s^2 \sim I_s$ , where  $I_s$  is the suppressor stimulation intensity, this explains the slow departure of the curves from zero suppression. As soon as  $R_s^2 \gg \mu$ , we observe the changed behavior

$$A_s(\text{int}) \sim \log \frac{R_s(2)^2}{R_s(1)^2} \approx \log \frac{I_s(2)}{I_s(1)}, \tag{12}$$

which explains the large constant spacings between the equi-dB-spaced response curves. For the last step, the suppressor-linear regime was necessary. When  $F_s$  is increased further, the suppressor enters its compressive nonlinear regime. This leads to  $R_s^2 \sim F_s^{2/3} \sim I_s^{\alpha/3}$  (note that in the suppressor-nonlinear regime,  $R_s^2 \sim I_s^\alpha$ , where still  $\alpha \approx 1$ ). We obtain

$$A_s(\text{cnl}) \approx \frac{1}{3} A_s(\text{int}) \tag{13}$$

showing, indeed, a suppressor efficacy decreased by a factor of three. As a last point, it is easily derived that the linear/compressive nonlinear transition point  $F_{t,\text{cnl}} = |\mu_{\text{eff},t}|^{3/2} = (|\mu - 2R_s^2|)^{3/2}$  changes its location as a function of the suppressor intensity, as found in the physiological and in the modelling data.

## 6. Discussion

Subcritical tuning of the Hopf amplifiers is an essential condition for the quality of our modelling. This ansatz is in contrast to critical tuning implemented by Magnasco [18], and Duke and Jülicher [19]. The question of (sub)critical tuning has recently been the object of extensive scientific discussions [20]. The fundamental problem with critical tuning for sustained single tones is that nonlinear responses  $R \sim F^{1/3}$  are obtained for the whole regime, irrespective of the stimulus size. This behavior, however, is in contradiction to the measured almost constant-gain regime for weak stimuli (below 20 dB in Fig. 3c, see also Ref. [12]). Moreover, at the point of active amplification, the amplifier bandwidth becomes exceedingly small ( $\Gamma_{3\text{ dB}} \sim F^{2/3}$ ),

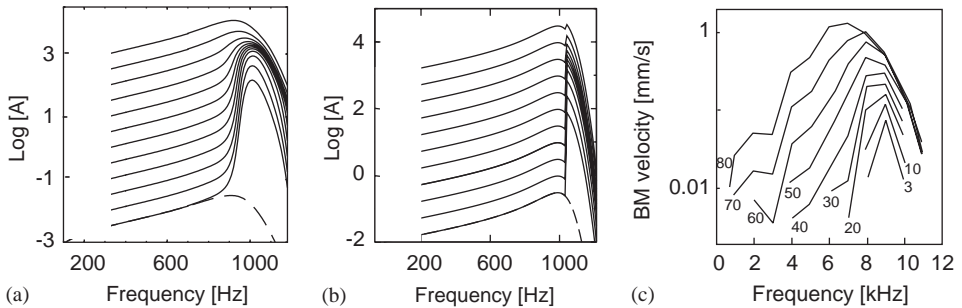


Fig. 3. Local BM frequency responses: (a) Hopf-cochlea model, Eq. (6), where longitudinal BM coupling has only been included. Dashed line: passive response (stimulus frequency:  $\omega/2\pi = 1000$  Hz). For adjacent lines, the stimulus intensity differs by 10 dB. (b) Discontinuous response emerges for quasi-critical ( $\mu \rightarrow \mu_{\text{crit}} = 0$ ) tuning (shown for  $\mu = -0.001$ ). (c) Experimental measurements [21].

which is the origin of unrealistic, discontinuous model responses [22] (see Fig. 3b, for a similar behavior see Ref. [18]).

From Eq. (4), it appears that in the presence of a second tone, a distinction between critical and subcritical tuning is unnecessary. This, however, is incorrect. For both tunings, the suppression threshold is given by  $R_s^2 \sim |\mu/2|$ , see Eq. (5). In the critical case, the transition point is determined by  $F_{t,cnl}^{crit} \approx 2^{3/2} R_s^3$ , whose lower bound is zero, obtained for  $F_s \rightarrow 0$ .  $F_{t,cnl}^{crit}$  therefore keeps changing for arbitrary weak suppressor intensities, implying that all BM input–output curves differ, and no accumulation occurs. Such a behavior, however, is not supported by the existing physiological data (e.g., Fig. 1b). In the subcritical case,  $|\mu_{eff}|$  cannot go below  $|\mu|$ , implying a stationary transition point  $F_{t,cnl}^{sub} = |\mu|^{3/2}$  for low suppressor intensities, in agreement with the observed accumulation of low-dB BM input–output curves. In fact, it is the subcritical tuning which is the origin of the excellent agreement between physiology and our model.

With the help of a biomorphic modelling approach we were able to give a detailed explanation of the nature of two-tone suppression. To achieve this, the subcritical tuning of Hopf amplifiers and their embedding in a biophysically detailed cochlea model was essential. The close correspondence between our biomorphically motivated model and the mammalian cochlea can also be used for the detailed simulation of hearing defects, providing a basis for quantitative non-contextual measurements of cochlear hearing damage.

## Acknowledgements

We thank M. Magnasco, T. Kohda, and W. Schwarz for beneficial exchanges on the subject, and the Swiss KTI and Phonak AG Hearing Systems for continued support.

## References

- [1] H.L.F. Helmholtz, *Die Lehre von den Tonempfindungen als physiologische Grundlage für die Theorie der Musik* (On the Sensations of Tones as the Physiological Basis for a Theory of Music), Vieweg, Braunschweig, 1863.
- [2] G. von Békésy, Zur Theorie des Hörens. Die Schwingungsform der Basilarmembran (On the theory of hearing. The vibration pattern of the basilar membrane), *Phys. Z.* 29 (1928) 793–810.
- [3] E. de Boer, Mechanics of the cochlea: modelling efforts, in: P. Dallos, A.N. Popper, R.R. Fay (Eds.), *The Cochlea*. Springer Handbook of Auditory Research, Springer, New York, 1996, pp. 258–317.
- [4] R.B. Patuzzi, P.M. Sellick, B.M. Johnstone, The modulation of the sensitivity of the mammalian cochlea by low frequency tones. III. Basilar membrane motion, *Hear. Res.* 13 (1984) 19–24.
- [5] L. Robles, M.A. Ruggero, N.C. Rich, Two-tone distortion in the basilar membrane of the cochlea, *Nature* 349 (1991) 413–414.
- [6] N.P. Cooper, W.S. Rhode, Basilar membrane mechanics in the hook region of cat and guinea-pig cochleae: sharp tuning and nonlinearity in the absence of baseline position shifts, *Hear. Res.* 63 (1992) 163–190.
- [7] C.D. Geisler, *From Sound to Synapse. Physiology of the Mammalian Ear*, Oxford University Press, Oxford, 1998.



- [8] R. Patuzzi, Cochlear micromechanics and macromechanics, in: P. Dallos, A.N. Popper, R.R. Fay (Eds.), *The Cochlea*. Springer Handbook of Auditory Research, Springer, New York, 1996, pp. 187–257.
- [9] D.T. Kemp, Evidence of mechanical nonlinearity and frequency selective wave amplification in the cochlea, *Arch. Otorhinolaryngol.* 224 (1979) 37–45.
- [10] M.A. Ruggero, L. Robles, N.C. Rich, Two-tone suppression in the basilar membrane of the cochlea: mechanical basis of auditory-nerve rate suppression, *J. Neurophysiol.* 68 (1992) 1087–1099.
- [11] W.S. Rhode, N.P. Cooper, Nonlinear mechanics in the apex of the chinchilla cochlea in vivo, *Auditory Neurosci.* 3 (1996) 101–121.
- [12] V.M. Egülüz, M. Ospeck, Y. Choe, A.J. Hudspeth, M.O. Magnasco, Essential nonlinearities in hearing, *Phys. Rev. Lett.* 84 (2000) 5232–5235.
- [13] P. Martin, A.J. Hudspeth, Compressive nonlinearity in the hair bundle's active response to mechanical stimulation, *Proc. Natl. Acad. Sci. USA* 98 (2001) 14386–14391.
- [14] E. Hopf, Abzweigung einer periodischen Lösung von einer stationären Lösung eines Differentialsystems (Separation of a periodic solution from a stationary solution of a system of differential equations), *Ber. Math.-Phys. Sächs. Akad. d. Wiss. Leipzig* 94 (1942) 1–22.
- [15] A. Kern, R. Stoop, Essential role of couplings between hearing nonlinearities, *Phys. Rev. Lett.* 91 (2003) 128101.
- [16] G.B. Whitham, *Linear and Nonlinear Waves*, Interscience Publishers, New York, 1999.
- [17] C.D. Geisler, C. Sang, A cochlear model using feed-forward outer-hair-cell forces, *Hear. Res.* 86 (1995) 132–146.
- [18] M.O. Magnasco, A wave traveling over a Hopf instability shapes the cochlear tuning curve, *Phys. Rev. Lett.* 90 (2003) 058101.
- [19] Th. Duke, F. Jülicher, The active traveling wave in the cochlea, *Phys. Rev. Lett.* 90 (2003) 158101.
- [20] A.W. Gummer, *Biophysics of the Cochlea. From Molecules to Models*, World Scientific, Singapore, 2003.
- [21] M.A. Ruggero, Responses to sound of the basilar membrane of the mammalian cochlea, *Curr. Opin. Neurobiol.* 2 (1992) 449–456.
- [22] Two-tone suppression experiments [8] suggest that hair cells over the extension of  $\approx 650\ \mu\text{m}$  contribute to active amplification. This would be hardly consistent with the narrow amplifier bandwidth of critical tuning. During nonstationary driving only,  $\mu$  may cross the critical point, e.g., in order to reduce the response time for follow-up signals.